

Software reliability design and modeling of flight control system for small UAV

JING FU¹, GUIWEI SHAO¹, JI HU¹, HUANQING CAI¹

Abstract. As the research and application of the helicopter in the transmission line inspection and the application of the continuous development, the security of the helicopter flight raised higher requirements, it is urgent to solve the problem of the safety of the helicopter in the power inspection process of the super low altitude flight. In this paper, the key techniques of the millimeter wave radar obstacle avoidance are studied, including the small target signal accumulation technology, the constant false alarm detection technology and the polarization detection technology, and in the theoretical analysis and field testing are very good results. Experiments show that this technique can effectively improve the detection ability of radar target mm, reduce the false alarm rate, greatly improves the safety of the power line patrol helicopter.

Key words. MMV radar Helicopter, Power line inspection system Small target detection

1. Introduction

In recent years, due to the continuous expansion of transmission lines, the routine patrol for transmission lines is more and more onerous. During the process of patrol and maintenance for the transmission lines, the maintenance automation of transmission lines will be more urgent for ensuring the safety and maintaining the efficiency. The patrol technology of transmission lines based on the helicopter comes into being, which puts more demands on the efficiency and safety of the helicopter patrol line.

The research on obstacle avoidance system of helicopter at abroad was carried out in the 60s of the last century and developed continuously in the following years. The MMW obstacle avoidance technology adopts FMCW or pulse and other systems and the function is also expanded from simple obstacle avoidance to obsta-

¹China Electric Power Research Institute, Wuhan Hubei, 430000

cle avoidance oriented, taking into account the development of navigation and so on. At present, helicopter anti-collision radar technology is equipped with a certain technology, and a variety of obstacle avoidance equipment had been developed successively via a variety of airborne systems since the 60s of the last century, including obstacle detection equipment and obstacle warning equipment, etc. [1] Presently, MMW obstacle avoidance radar featuring with large broadband, small volume and lightweight comparatively meets the airborne, of which the wave length is between 1~10mm [2]. Several typical MMW anti-collision radars abroad are as follows: SAIGA researched by MARCEL DASSALILT, U-band anti-collision radar researched by AEG-TELEFUNKEN in the 80s of last century, Ka-band Oasys anti-collision radar researched by the Canada Amphitech in 2000 [3]. Many domestic institutes are developing helicopter obstacle avoidance system, such as research on MMW helicopter obstacle avoidance radar by the 10th Research Institute of China Electronics Technology Group Corporation, technology accumulation in laser radar of the 27th Research Institute of China Electronics Technology Group Corporation, and in addition, the 54th Research Institute of China Electronics Technology Group Corporation and Southeast University and other organizations have achieved good results in research. However, there are a few reports regarding transmission line patrol presently.

The use of MMW obstacle avoidance radar in the helicopter patrol line system will better improve the efficiency and safety of Helicopter patrol line system to open wider application prospects. The helicopter transmission line patrol system has been applied to the actual power production process, as it can not avoid the emergency obstacles in general and it is likely to collide with the cross transmission lines ahead if the flying height of the helicopter is not high, so it is necessary to develop a set of obstacle avoidance system for helicopter patrol line.

2. System composition

The MMW radar obstacle avoidance system shall be applied to the patrol system of electrical helicopter to achieve the obstacle avoidance of helicopter for the obstacles such as transmission ground wires, towers, elevated antennas water towers, oil platforms, steel cables and isolated structures in patrolling. The operation task of the system is as follows:

MMW radar obstacle avoidance system can automatically report the obstacles within the warning distance in each direction from patrolled route under complex meteorological conditions and send to the flight control system for obstacle avoidance decision. The obstacle avoidance sensor system is installed in the helicopter's 8 horizontal directions and 1 vertical direction, respectively for system switching. The specific structure of each system is shown below:

Each system adopts broadband linear frequency modulation continuous wave (WLFMCW) radar system, consisting of two parts: system based on DDS+PLL frequency multiplication technology and MMW and data acquisition and processing system based on FPGA technology, as follows:

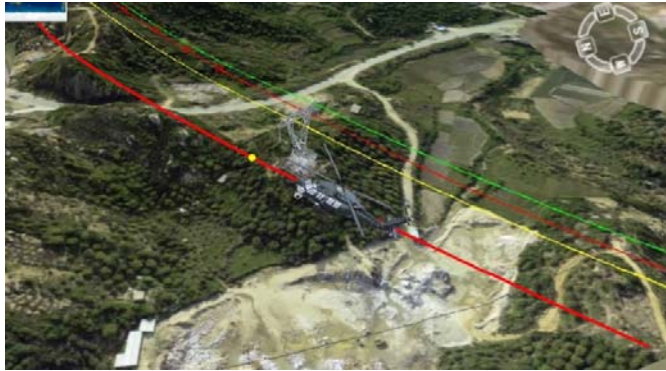


Fig. 1. Operation task picture

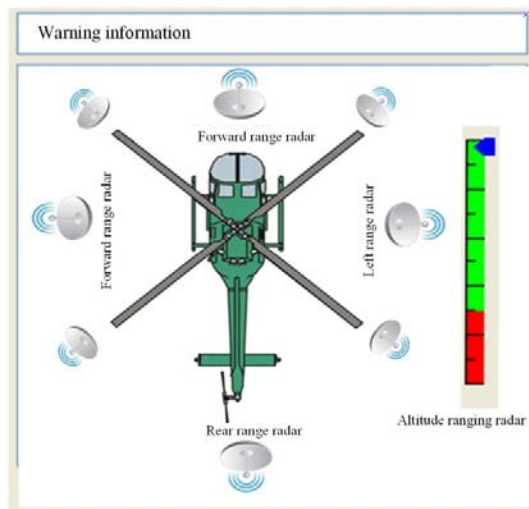


Fig. 2. Composition for setting of specific system on helicopter

3. Analysis on key technology of MMW obstacle avoidance radar system

During the detection by radar system, one of the most important parameters is radar-cross section (RCS). Regarding the transmission line patrol system of helicopter, the ground background of radar beam irradiation is quite different during flight, such as forests, mountains, lakes, rivers, etc. Compared with general trees and mountains and other obstacles, the transmission lines have a small RCS that is difficult to be detected by the radar, so which poses a great threat for the flight of helicopter. The Section mainly introduces a kind of detection technology for target with small RCS to improve the obstacle avoidance capacity of helicopter.

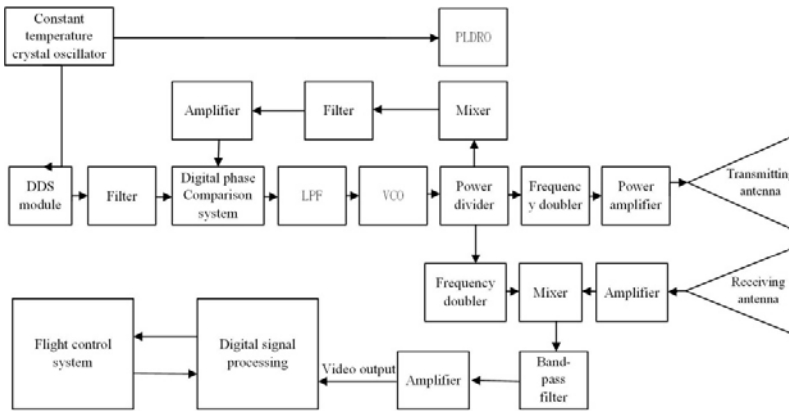


Fig. 3. General system composition

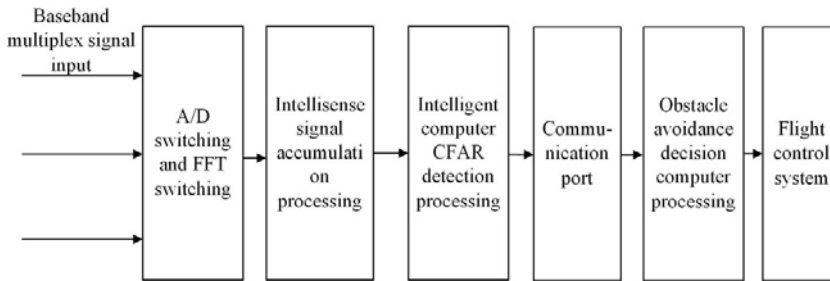


Fig. 4. Composition of baseband signal processing system

3.1. Phase-coherent accumulation and noncoherent integration method

Signal-noise ratio (SNR) is a key indicator for the radar signal detection [4], the higher the SNR of target echo is, the better the detection effect of the radar detection is. In the field of radar signal detection, a general method to improve the echo SNR is the signal accumulation method, including two types: phase-coherent accumulation and noncoherent integration method.

(1) Phase-coherent accumulation method: before the envelope detection of signals, phase-coherent accumulation is first used to improve the SNR. The method is to add the amplitude and phase of all echo pulses at the same range gate. If there is M echo pulse(s) in the range gate, the SNR can be improved to M time(s) of the original signal.

(2) Noncoherent integration method: before the envelope detection of signals, cross-cycle accumulation shall be implemented on the M echo pulse(s) in the same range gate, and the phase of accumulated phase is lost and only includes the amplitude information of the original signal. As the loss of phase information, SNR can be improved between \sqrt{M} and M .

The difference between noncoherent integration and phase-coherent accumulation

is called accumulation loss, usually referred to as L . The accumulation loss is defined as the ration of detection factor of noncoherent integration and phase-coherent accumulation in the case of that the false alarm probability p_{fa} is controlled within a certain range for some detection probability. The empirical formula proposed by Peebles is shown in Formula (1) to control the improved factor within 0.8dB.

$$I(M)_{dB} = 6.79(1 + 0.235P_D) \left(1 + \frac{\log(1/p_f)}{46.6}\right) \log(M) \times \left(1 - 0.141 \log(M) + 0.0183(\log(M))^2\right). \quad (1)$$

With respect to different p_f and p_D value, the relation curve between the noncoherent integration loss and the number of pulse can be obtained. As shown in Fig. 5, the noncoherent integration loss is increased with the increase of the number of pulse accumulation and decreased with the increase of SNR.

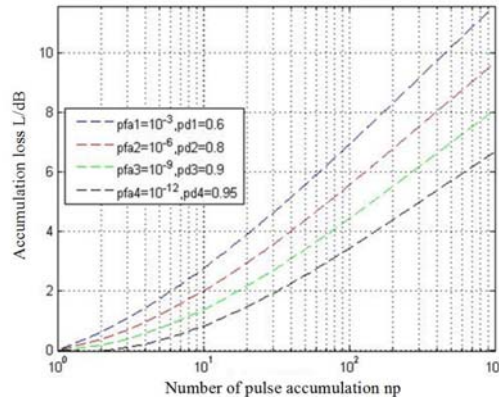


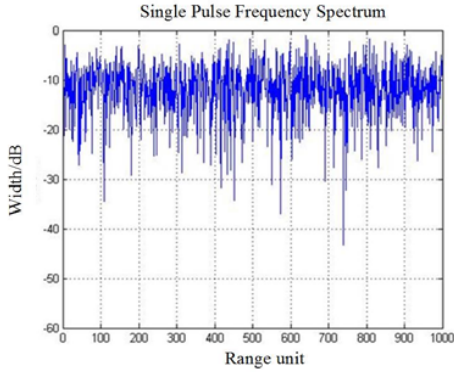
Fig. 5. Noncoherent integration loss curve

Simulation analysis: Simulation of phase-coherent accumulation and noncoherent integration are carried out by Matlab software, where the parameters are set as follows:

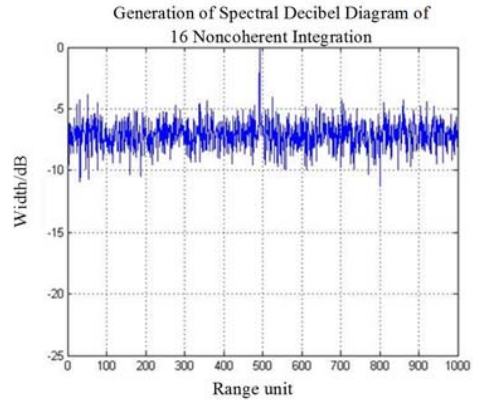
- (1) Echo SNR: SNR=-20dB.
- (2) Wavelength of radar transmission signal: 8mm.
- (3) FM time width: 200us.
- (4) Signal bandwidth: 400MHz.
- (5) Sampling points: 2048.
- (6) Sampling frequency: 20MHz

Simulation figure is shown in Fig. 6.

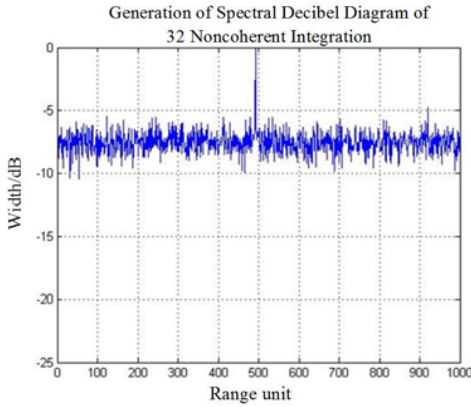
The following conclusions are obtained from the simulation results of Fig.6: first, the single periodic target echo signal is completely covered by noise due to the low SNR, as shown in Figure 6 (a). Second, whether the use of phase-coherent accumulation or non-coherent integration, can improve the SNR of the echo signal,



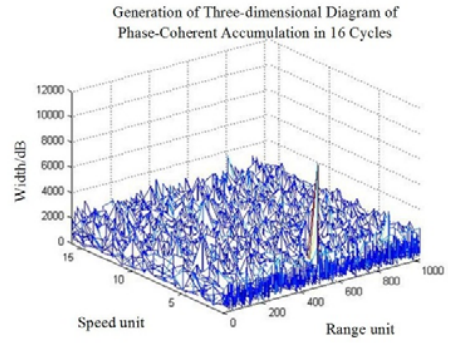
(a) Spectral decibel diagram of single cycle



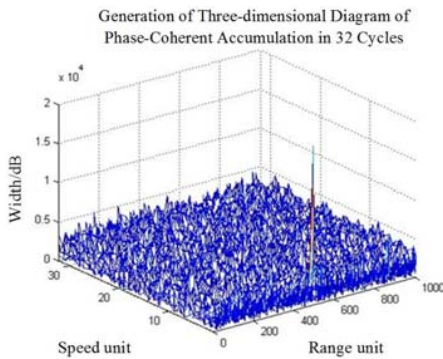
(b) Spectral decibel diagram of 16 noncoherent integration



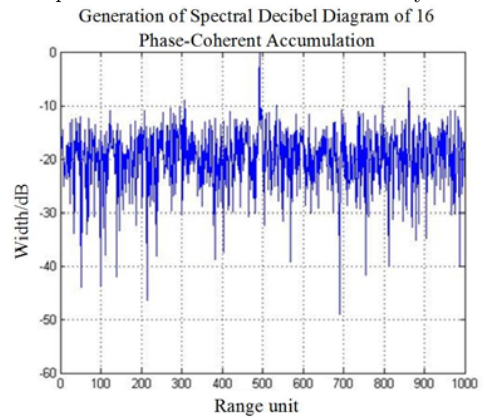
(c) Spectral decibel diagram of 32 noncoherent integration



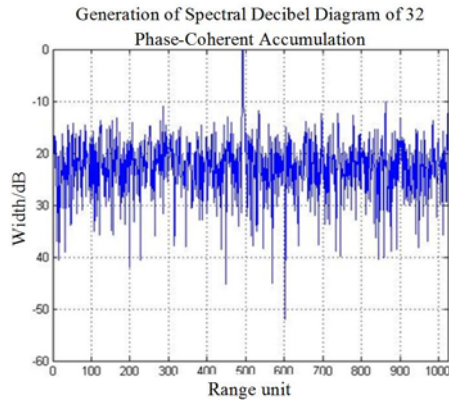
(d) Three-dimensional diagram of phase-coherent accumulation in 16 cycles



(e) Three-dimensional diagram of phase-coherent accumulation in 32 cycles



(f) Spectral decibel diagram of 16 phase-coherent accumulation



(g) Spectral decibel diagram of 32 phase-coherent accumulation

Fig. 6. Diagram of phase-coherent accumulation and noncoherent integration of echo signal

thereby improving the detection rate. Third, the improvement degree of SNR is closely related to the number of phase-coherent accumulation (namely accumulation time), and the more the number of phase-coherent is, the higher the SNR is.

3.2. Constant false-alarm detection method

During the target detection by radar, as there are many kinds of targets in the scanning area, such as vegetation, mountains, lakes, buildings and other targets, therefore, the echo signal of the target to be checked will be covered by the noise of the above target. So it is necessary to preset the false-alarm probability and the targets shall be detected under this probability. The detection threshold [5] shall be set by constant false-alarm detection method to minimize the influence of noise signal on the false-alarm probability, of which the detection threshold shall be determined in accordance with the following methods: (1) fixed value; (2) average amplitude based on external disturbance; (3) partial prior information calculated and distributed in accordance with interference signal; (4) inspection according to assumption. Hereon, we only discuss adaptive constant false-alarm detection method.

The structure of constant false-alarm rate (CFAR) detector is shown in Fig. 7. The sampling sequence of clutter is obtained by square-law detection to enter into the shift register with length of $N+1$ orderly, which forms CFAR sliding window reference unit, where D refers to the detection unit, located in the center of sliding window. Based on the N clutter sample(s) in the front and rear reference window, the clutter power is obtained, which can be used for setting the thresholds for detecting targets.

With respect to CA-CFAR detector, the detection performance for multiple targets is poor [6] and there are a lot of false alarms at the edge of the clutter signal. Regarding this point, it can be improved in accordance with the model of the clutter, of which the main methods include SOCA-CFAR and GOCA-CFAR. To compare

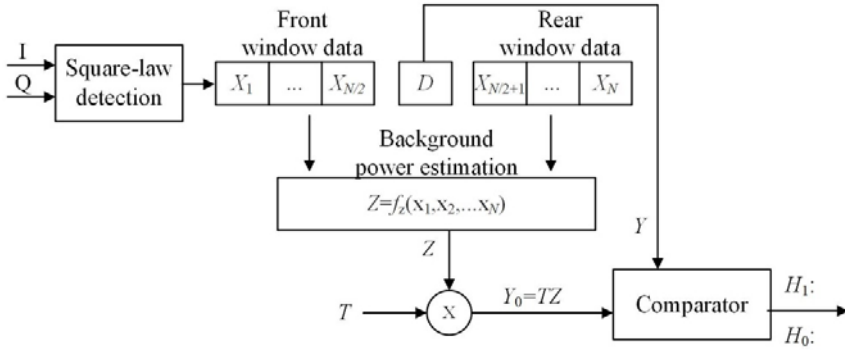


Fig. 7. Structure diagram of typical CFAR detector

the detection performance of different detector, the simulation experiment is carried out. Compared with CA-CFAR, SO-CFAR is capable of detecting two close targets and the targets near the clutter edge, as shown in Fig. 8. GO-CFAR can control CFAR in the edge of clutter and the strong target covers the weak target, as shown in Fig. 9. These two methods, while improving, will also bring some additional detection losses.

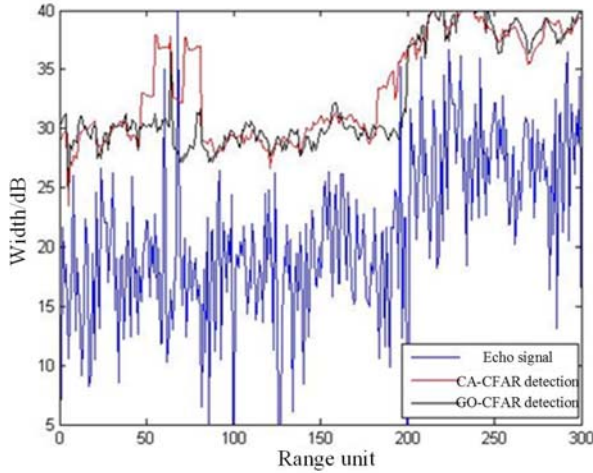


Fig. 8. CA-CFAR and SO-CFAR detection

In the airborne obstacle avoidance radar system, the target background to be detected includes the earth, vegetation, and mountains, and these clutter will produce dramatic changes in space and time, of which general CA-CFAR detection has limitations in clutter edge detection. The above discussions show that GO-CFAR detection can satisfy the requirement of constant false-alarm processing and the GO-CFAR ideal detection block diagram is shown in Fig. 10.

As a whole, GO-CFAR is superior to CA-CFAR detector. At different noise

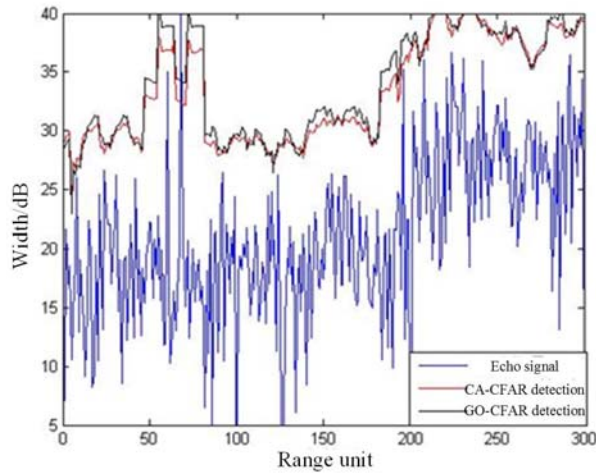


Fig. 9. CA-CFAR and GO-CFAR detection

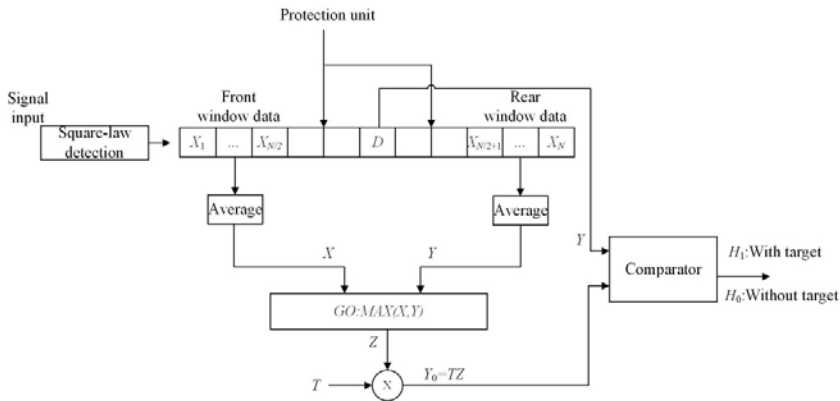


Fig. 10. GO-CFAR detection block diagram

ratio, the false-alarm ratio of the GO-CFAR detector is basically constant when the clutter is located in the rear reference window [8]. While implementing the obstacle avoidance by radar, because of the variety of objects in the scanning area, including vegetation, alpine, lakes, buildings and other different targets, the change of clutter is very obvious and the CA-CFAR detection method does not apply to this situation, therefore, GO-CFAR detection method is relatively proper, of which the detection block diagram is shown in Fig. 10.

3.3. Polarization detection algorithm

For the transmission ground wire, the echo will be weak, even far below the ground clutter signal when the difference between incident angle and the vertical angle of the radar wave is too large. So the signal to clutter ratio of the echo signal is

very low, which makes the transmission ground wire difficult to detect. The method of improving SNR mentioned above is of no use in the case of low signal to clutter, therefore, polarization variable radar shall be used to improve the signal to clutter ratio combined with statistical algorithm. Literature [9] shows that for the radar with CO polarization and orthogonal polarization, the back scattering direction of the electromagnetic wave after passing through medium surface is symmetric but not related, that is,

$$\langle S_{hh}S_{vh}^* \rangle = \langle S_{vv}S_{vh}^* \rangle = 0. \quad (2)$$

where, $\langle \cdot \rangle$ means all numerical value averaging operator. Hereon, arithmetic formula represented by expression (3.35) of operator \mathcal{L} is introduced to better represent the useful signals covered by noise by statistic value of the clutter. Where, S_c and S_s respectively refers to the measurement scattering matrix of the clutter and useful signal. There is,

$$\langle \mathcal{L}(S_c) \rangle = 0. \quad (3)$$

When the incident angle of radar wave is fixed, the backscattering of the ideal transmission line model is determined, so orthogonal polarization and co-polarization are completely related. However, in practical, the transmission ground wire is not an ideal model and the angle of incidence of radar antenna patterns also varies slightly. The actual experiments show that, whether it is amplitude or phase, σ_{vv} and σ_{vh} of the transmission ground wire is almost completely related, which can be used to detect the high voltage wire, that is,

$$\mathcal{L}(S) = \mathcal{L}(S_c + S_s) \neq 0. \quad (4)$$

In literature [10], regarding the different background of wood and asphalt pavement, the value of the $\langle S_{vv}S_{vh}^* \rangle$ is measured respectively. The measured results show that the value of $\langle S_{vv}S_{vh}^* \rangle$ increases obviously when there is transmission ground wire. Compared with HH and HV polarization, in the deviation from the angle with large vertical range, the signal strength obtained by VV polarization is large, which can produce major orthogonal polarization backscattering. Based on the calculation of $\langle S_{vv}S_{vh}^* \rangle$, instead of calculating $\langle |S_{vv}S_{vh}^*| \rangle$, it can suppress clutter and improve signal to clutter ratio and improve the probability to detect the transmission ground wire in the case of strong clutter.

Under a certain false-alarm probability, to achieve designed detection probability, the proper threshold value is required to be set. Define variable γ as correlation coefficient of VV and HV channel.

$$\gamma = \frac{\langle S_{VV}S_{HV}^* \rangle}{\sqrt{\langle |S_{VV}|^2 \rangle \langle |S_{HV}|^2 \rangle}}. \quad (5)$$

It is assumed that the stochastic process is ergodic, the spatial mean can be used as an approximation to compute the coherent estimate and the threshold value is determined by the detection probability and false-alarm probability, of which the detection probability is determined by the following three factors: backscatter level

of ground wire, backscatter coefficient and number of samples sampled.

Where, the backscatter coefficient of HH and HV polarization is relatively closed, and the intensity of the background clutter and its statistical characteristics determine the detection probability and false-alarm probability of the transmission ground wire. The co-polarization component and orthogonal polarization component of trees are more obvious, and the latter is only 4-5dB higher than the former.

The correlation coefficient of orthogonal polarization and co-polarization for clutter and transmission ground wire is the basis of the algorithm in the paper. During the process of calculating the correlation coefficient, the average estimate of a finite observation sample is considered as a random variable, generally, the mean of this random variable is the same, and the variance is small. When the coherence coefficients are estimated, the average estimate is always greater than the coherence value, namely $\langle \hat{\gamma} \rangle > \gamma$. When the coherence value of clutter is 0, the average estimate is always greater than 0. The detection probability and false-alarm probability shall be quantified by the probability density function (PDF) of coherent estimate of transmission ground wire and clutter.

(1) With respect to the clutter, assuming that it obeys the Gauss distribution, the PDF of coherent estimate of orthogonal polarization and co-polarization is:

$$p(\hat{\gamma}) = 2(N-1)(1-\gamma^2)^N \times \hat{\gamma}(1-\hat{\gamma}^2)^{N-2} F(N, N; 1; \gamma^2 \hat{\gamma}^2), \quad (6)$$

where, γ means the coherence value, N refers to the number of samples and F represents the hypergeometric function. As the coherence value of clutter signal $\gamma = 0$, the PDF can be represented as:

$$p(\hat{\gamma}) = 2(N-1)\hat{\gamma}(1-\hat{\gamma}^2)^{N-2}. \quad (7)$$

(2) Regarding transmission ground wire, the coherence value of the sampling point is the function of the backscatter coefficient of transmission ground wire and clutter, namely:

$$\gamma = \frac{|\sigma_{VV,HV}^p|}{\sqrt{(\sigma_{VV}^o A + \sigma_{VV}^p)(\sigma_{HV}^o A + \sigma_{HV}^p)}}. \quad (8)$$

where, σ_{VV}^p refers to the RCS of VV of transmission ground wire for image point, σ_{HV}^p refers to the RCS of HV of transmission ground wire for image point, $\sigma_{VV,HV}^p = 4\pi S_{VV} S_{HV}^*$ is the cross-correlation value of backscatter of VV and HV , A refers to the area of pixel and σ_{VV}^o and σ_{HV}^o represents the backscatter coefficient of the clutter. The first and two moments of the estimate of the coherence coefficients are:

$$\begin{aligned} \langle \hat{\gamma} \rangle &= \frac{\Gamma(N)\Gamma(3/2)}{\Gamma(N+1/2)} {}_3F_2(3/2, N, N; N+1/2, 1; \gamma^2)(1-\gamma^2)^N, \\ \langle \hat{\gamma}^2 \rangle &= \frac{1}{N} {}_3F_2(2, N, N; N+1, 1; \gamma^2)(1-\gamma^2)^N. \end{aligned} \quad (9)$$

where, Γ represents gamma function and ${}_pF_q$ is generalized hypergeometric series. As ${}_3F_2(2, N, N; N + 1, 1; 0) = 1$, the mean of coherent estimate for the clutter and its expression of second moment can be simplified to:

$$\langle \hat{\gamma} \rangle = \frac{0.8862\Gamma(N)}{\Gamma(N + 1/2)}, \quad \langle \hat{\gamma}^2 \rangle = \frac{1}{N}. \tag{10}$$

The mean and second moment are only functions of N. The parameters values are expanded by gamma function and the mean of coherent estimate when $N > 10$ is:

$$\langle \hat{\gamma} \rangle = \frac{0.8862}{\sqrt{N}}. \tag{11}$$

The standard variance in this case is approximately $0.462/\sqrt{N}$. False-alarm probability is

$$P_{FAR} = 2(N - 1) \int_{\gamma_T}^1 \hat{\gamma}(1 - \hat{\gamma}^2)^{N-2} d\hat{\gamma}. \tag{12}$$

Then

$$\gamma_T = \sqrt{1 - FAR^{\frac{1}{N-1}}}. \tag{13}$$

Detection probability is

$$P_{PD} = 1 - 2(N - 1)(1 - \hat{\gamma}^2)^N \times \int_0^{\gamma_T} \hat{\gamma}(1 - \hat{\gamma}^2)^{N-2} F(N, N; 1; \gamma^2 \hat{\gamma}^2) d\hat{\gamma} \tag{14}$$

P_{PD} can be expanded as follows based on hypergeometric equation series:

$$P_{PD} = 1 - (N - 1)(1 - \hat{\gamma}^2)^N \times \sum_{k=0}^{\infty} \sum_{j=0}^{N-2} \left(\frac{(N + k - 1)! \gamma^k}{(N - 1)! k!} \right)^2 \times \frac{(N - 2)!}{(N - j - 2)! j! (j + k + 1)} \times \left(1 - FAR^{\frac{1}{N-1}} \right)^{(j+k+1)}. \tag{15}$$

Generally, γ_T is a fairly small number ($\gamma_T < 0.2$).

If the number of sampling point $N=300$, the PDF of the clutter and transmission ground wire is shown in Fig. 11, of which the coherence value of the clutter $\gamma = 0$, and the coherence value of the transmission ground wire $\gamma = 0.2$. For different false-alarm probabilities, the relation between threshold value and the number of sampling point N is shown in the Fig. 12.

4. Analysis on experiment results

We carried out a trial flight test of the helicopter patrol system at an experimental base. MMW obstacle avoidance radar system can detect millimeter -level

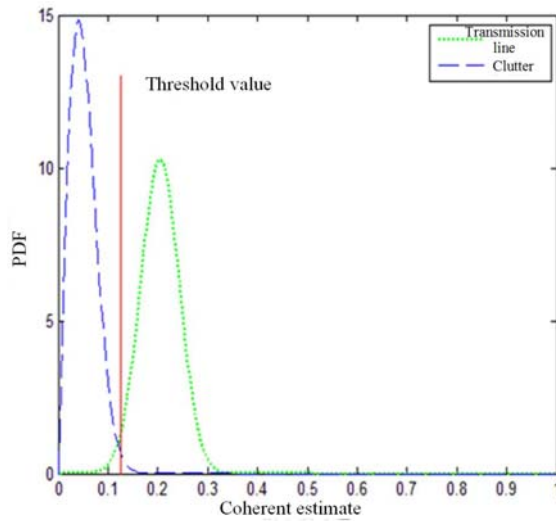


Fig. 11. PDF of coherent estimate for transmission ground wire and clutter

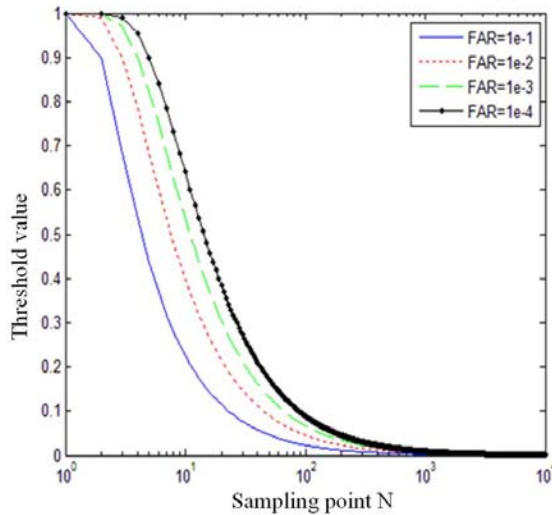


Fig. 12. Relation curve of number of sampling point N and threshold value under different false-alarm probabilities

transmission cables very well and the ranging accuracy is 0.4 meters, where the transmission line can be imaged in distance and two parallel wires of 1 meter apart can be distinguished in the horizontal direction of distance. In the system, the target information detected by the helicopter obstacle avoidance radar is sent to the flight control system through the UART module and the helicopter control system is controlled by the flight control system.

In the experiment, flight state control of helicopter is realized. For example,

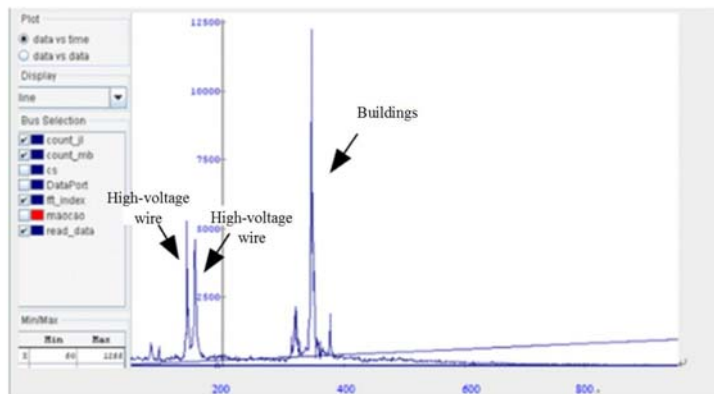


Fig. 13. Transmission line results detected in pitch angle on obstacle avoidance system

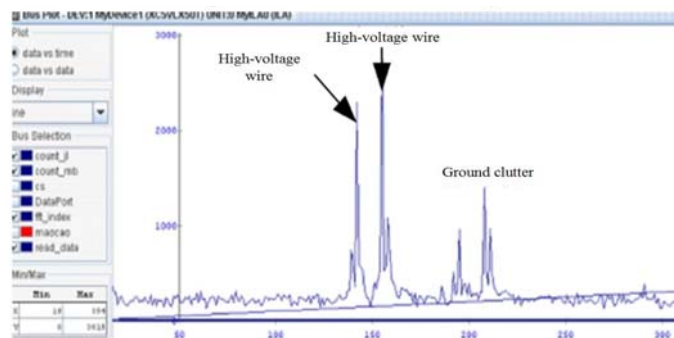


Fig. 14. Transmission line results detected in pitch angle under radar of obstacle avoidance system

when a flight encounters obstacles such as transmission lines, earth wires, telegraph poles, trees, etc, the obstacle avoidance system prompts the alarm information in the corresponding direction. In the testing, the system detects the data reliably, and can well adapt to the airborne electromagnetic environment and the vibration and impact environment. The results detected in the true environment are shown in the Fig. 13 and Fig. 14, showing that small target devices such as transmission high-voltage wire are easier to be detected.

References

- [1] ULABY, F.T.: (1990) *C.Elachi. Radar polarimetry for Geoscience Applications*. Artech House, Dedham MA.
- [2] MOONSOO PARK: (2003) Millimeter-Wave Polarimetric Radar Sensor for Detection of Power Lines in Strong Clutter Background.
- [3] TOUZI, R. AND A.LOPES.: (1996) *Statistics of the Stokes parameters and of*

- the complex coherence parameters in one-look and multi-look speckle field.* IEEE Trans.Geosci.Remote Sensing. 34:519-532
- [4] YAMAGUCHI H, KAJIWARA A, HAYASHI S: (1999) *Radar cross section measurements for collision avoidance with power transmission line at millimeter-wave frequencies*[C]// Radar Conference, 1999. the Record of the. IEEE, 1999:148-153.
 - [5] LV, Z., TEK, A., DA SILVA, F., EMPEREUR-MOT, C., CHAVENT, M., & BAADEN, M.: (2013). *Game on, science-how video game technology may help biologists tackle visualization challenges.* PloS one, 8(3), e57990.
 - [6] LV, Z., HALAWANI, A., FENG, S., LI, H., & RÉHMAN, S. U.: (2014). *Multimodal hand and foot gesture interaction for handheld devices.* ACM Transactions on Multimedia Computing, Communications, and Applications (TOMM), 11(1s), 10.
 - [7] WEISEN PAN, SHIZHAN CHEN, ZHIYONG FENG: (2013) *Automatic Clustering of Social Tag using Community Detection.* Applied Mathematics & Information Sciences, 7(2): 675-681.
 - [8] YINGYUE ZHANG, JENNIFER W. CHAN, ALYSHA MORETTI, AND KATHRYN E. UHRICH: (2015) *Designing Polymers with Sugar-based Advantages for Bioactive Delivery Applications,* Journal of Controlled Release, 219, 355-368.
 - [9] YINGYUE ZHANG, QI LI, WILLIAM J. WELSH, PRABHAS V.: Moghe, and Kathryn E. Uhrich (2016) *Micellar and Structural Stability of Nanoscale Amphiphilic Polymers: Implications for Anti-atherosclerotic Bioactivity,* Biomaterials, 84, 230-240.
 - [10] JENNIFER W. CHAN, YINGYUE ZHANG, AND KATHRYN E. UHRICH: (2015) *Amphiphilic Macromolecule Self-Assembled Monolayers Suppress Smooth Muscle Cell Proliferation,* Bioconjugate Chemistry, 26(7), 1359-1369.

Received May 7, 2017

